Wet scavenging limits the detection of aerosol effects on precipitation

E. Gryspeerdt[1,2], P. Stier[1], B. A. White[1], and Z. Kipling[1]

[1]Department of Physics, University of Oxford, UK
[2]Institute for Meteorology, Universität Leipzig, Germany

Correspondence to: E. Gryspeerdt
(edward.gryspeerdt@uni-leipzig.de)

Abstract. Satellite studies of aerosol–cloud interactions usually make use of retrievals of both aerosol and cloud properties, but these retrievals are rarely spatially co-located. While it is possible to retrieve aerosol properties above clouds under certain circumstances, aerosol properties are usually only retrieved in cloud free scenes. Generally, the smaller spatial variability of aerosols compared to clouds reduces the importance of this sampling difference. However, as precipitation generates an increase in spatial variability, the imperfect co-location of aerosol and cloud property retrievals may lead to changes in observed aerosol-cloud-precipitation relationships in precipitating environments.

In this work, we use a regional-scale model, satellite observations and reanalysis data to investigate how the non-coincidence of aerosol, cloud and precipitation retrievals affects correlations between them. We show that the difference in the aerosol optical depth (AOD)-precipitation relationship between general circulation models (GCMs) and satellite observations can be explained by the wet scavenging of aerosol. Using observations of the development of precipitation from cloud regimes, we show how the influence of wet scavenging can obscure possible aerosol influences on precipitation from convective clouds. This obscuring of aerosol-cloud-precipitation interactions by wet scavenging suggests that even if GCMs contained a perfect representation of aerosol influences on convective clouds, the difficulty of separating the "clear-sky" aerosol from the "all-sky" aerosol in GCMs may prevent them from reproducing the correlations seen in satellite data.

1 Introduction

Aerosols have an important influence on cloud properties by providing cloud condensation nuclei (CCN). An increased number of CCN can lead to an increase in cloud droplet number concentration

and a reduction in droplet size (Twomey, 1974), which in turn has been hypothesised to lead to a reduction in precipitation (Albrecht, 1989). Theoretical (Williams et al., 2002; Rosenfeld et al., 2008; Stevens and Feingold, 2009) and modelling studies (Khain et al., 2005; Tao et al., 2007) have suggested that under certain conditions, this liquid-phase suppression of precipitation may lead to an invigoration of convective clouds through the additional release of the latent heat of freezing. An invigoration of convective clouds may in turn lead to an increase in precipitation from the cloud in later stages of its lifecycle.

Observational studies have detected positive correlations between aerosols and precipitation that might indicate aerosol invigoration of convective clouds (Lin et al., 2006; Li et al., 2011; Koren et al., 2012; Niu and Li, 2012; Gryspeerdt et al., 2014b). These studies generally show an increase in precipitation with increase in a CCN proxy (aerosol optical depth (AOD – Andreae and Rosenfeld, 2008) or aerosol index (AI – Nakajima et al., 2001). However, given that precipitation is responsible for the removal of the majority of atmospheric aerosol (Textor et al., 2006), wet scavenging might be expected to generate a strong negative correlation between AOD and precipitation. Although this negative correlation is not observed in satellite studies, it can be observed in global models (e.g. Fig. 1c), especially in regions of high precipitation.

Correlations between aerosol and cloud properties have been shown to be strongly influenced by meteorological covariation and retrieval errors (Zhang et al., 2005; Mauger and Norris, 2007; Wen et al., 2007; Chand et al., 2012). Evidence from global models suggests that the positive correlation between AOD and precipitation rate (Fig. 1a) is largely due to aerosol hygroscopic growth, resulting in an AOD covariation with relative humidity (Boucher and Quaas, 2012; Grandey et al., 2014). Along with aerosol hygroscopic growth, retrieval errors such as cloud contamination of AOD retrievals (Zhang et al., 2005) can also lead to a positive correlation between AOD and cloud properties. Retrieval errors and aerosol hygroscopic growth together have been shown to be responsible for the majority of the positive correlation between AOD and cloud fraction (CF) (Quaas et al., 2010; Chand et al., 2012; Grandey et al., 2013). Influences on the AOD–CF correlation are particularly important, as the strong correlation between CF and other cloud parameters (including precipitation) can generate correlations between AOD and these cloud parameters (Gryspeerdt et al., 2014a).

While observational studies have shown an increase in precipitation with increasing AOD, this correlation is not always found when using general circulation models (GCMs). The difference between models and observations is demonstrated in Fig. 1, where each of the subplots shows the difference in precipitation rate between the highest and lowest quartiles of AOD over five years of data. Figs. 1a,b use precipitation data from the TRMM merged precipitation dataset (Huffman et al., 2007) between 2003 and 2007, but different AOD products. Fig. 1a uses the MODIS AOD product (Remer et al., 2005) and Fig. 1b using the MACC reanalysis AOD (Morcrette et al., 2011). For comparison, the same analysis is performed on a 5-year simulation from the HadGEM3-UKCA GCM (Mann et al., 2014), showing similar results to the ECHAM-HAM GCM (Grandey et al., 2014).
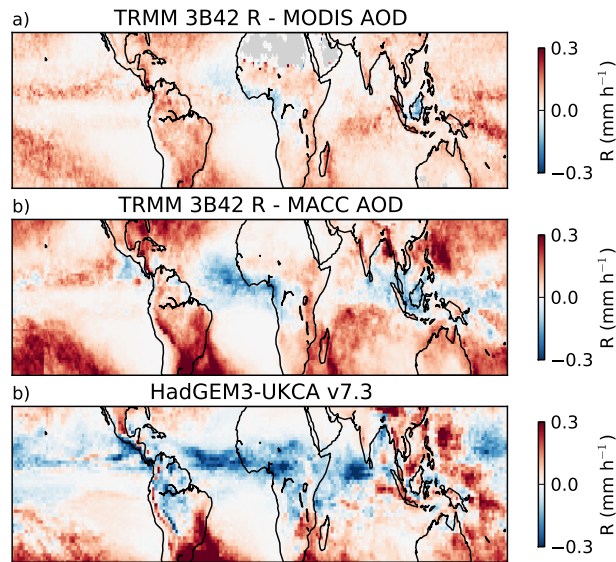
Figure 1. The difference in the TRMM merged precipitation rate between the highest and lowest AOD quartiles when using (a) MODIS and (b) MACC AOD between 2003 and 2007. c) The same as (a) but using 5 years of HadGEM-UKCA precipitation and AOD. Red(blue) indicates an increase(decrease) in precipitation for the high AOD population.

Meteorological covariations partially disguise the negative relationship between AOD and pre-

60 cipitation that exists as the result of the wet scavenging of aerosol (Quaas et al., 2010; Grandey et al., 2014). However, as models are expected to reproduce covariations between aerosol and cloud properties, these covariations are unlikely to be the cause of the difference in the AOD–precipitation correlation between models and observations seen in Fig. 1. Previous studies have suggested that the difference is due to the different sampling between models and observations (Grandey et al., 2013,

65 2014). Understanding the impact of sampling on modelled and observed aerosol–cloud–precipitation correlations (Fig. 1) is important for determining the strength of the aerosol influence on clouds and precipitation.

Whilst there are some instruments (e.g. Winker et al., 2007) and algorithms (Jethva et al., 2014) that can retrieve the properties of aerosols above or below cloud, the most commonly used satellite

70 retrievals of aerosol properties are only performed in cloud-free skies. On the other hand, GCMs are able to determine the aerosol concentration in cloudy skies, and so can determine the AOD in cloudy or precipitating scenes. This variation in sampling means that the aerosol seen by a model or the "all-sky" aerosol may be very different from the satellite sampled or "clear-sky" aerosol, especially in strongly precipitating locations. Almost all observational studies of aerosol–cloud–precipitation

75 interactions use "clear-sky" sampling and studies using GCMs use the "all-sky" sampling. This

3

means it is vital to account for the discrepancies caused by the differing sampling if observational studies are to be used in constraining aerosol–cloud interactions in GCMs.

Most GCMs only carry the "all-sky" aerosol between timesteps, meaning that GCMs effectively assume that each gridbox is well mixed over a period equal to that of the model timestep (usually 80 10–30 minutes). Within this limitation, GCMs take some steps to determine a "clear-sky" AOD, taking into account the wet scavenging that has occurred during a model timestep to diagnose a "clear-sky" AOD. Some GCMs also take account of the variation in relative humidity (RH) between in-cloud and out-of-cloud locations when diagnosing the AOD (e.g. Stier et al., 2005), resulting in a difference between the "all-sky" and the "clear-sky" AOD within a GCM gridbox. However, as wet 85 scavenging affects the CCN population rather than just the AOD, accounting for RH variations does not account for the underlying CCN (and AOD) variations caused by precipitation. Throughout this work we refer to the difference in sampling between GCMs and satellites, but any process which prevents the separation of "clear-sky" aerosol from "all-sky" aerosol in GCMs (such as assumptions about mixing) can generate these results.

90 This work focuses on possible aerosol interactions with precipitation from convective clouds, using regional-scale models, reanalysis and satellite data to investigate the impact of aerosol sampling on the AOD–precipitation relationship. A high resolution model is used to examine the impact of only retrieving AOD in cloud free locations on the mean AOD. A composite convective system from this model is used to examine the impact of heavily precipitating systems on AOD in the neighbour- 95 hood of these systems and to investigate the detectability of aerosol–cloud interactions by satellites. We use the precipitation development method of Gryspeerdt et al. (2014b) together with satellite and re-analysis (to provide a model-like observational product) AOD products to investigate the link between aerosol and precipitation in observations while accounting for meteorological covariations. Combining the results from these methods, we show how wet scavenging can impact the detectability 100 of aerosol influences on precipitation from convective clouds.

2 Methods

2.1 Model setup

We use v3.4.1 of the Weather Research and Forecasting (WRF)-Chem model (Grell et al., 2005) with a 10 km horizontal grid length. Although this is not sufficient to resolve small-scale convective 105 features, it is able to resolve the larger precipitating systems that impact aerosol in this region. A model grid length of 10 km requires a cumulus parametrisation, in this study we use the Grell 3D ensemble scheme (Grell, 2002). We use 30 vertical levels and the standard WRF stretched vertical grid, with grid spacing of about 100m in the lower levels, increasing towards the upper levels. This provides sufficient resolution to resolve the vertical structure of the aerosol and precipitation within 110 our study region. To provide the atmospheric heat and moisture tendencies, microphysical rates
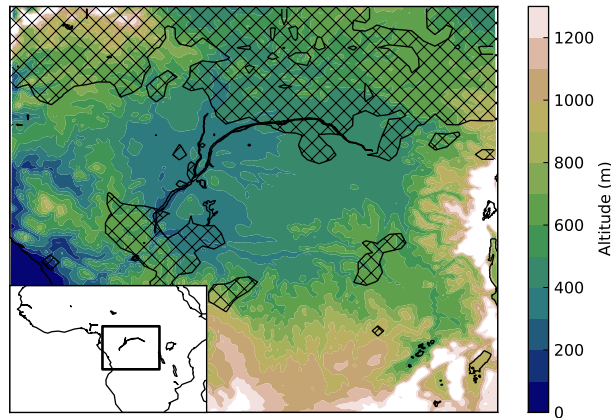
Figure 2. The domain used for the WRF-Chem simulations in this study. The colours indicate the altitude and the hatched areas indicate regions where MODIS detects more than one fire per $5,000\,km^2$ over the simulation time period. The inset shows the domain location over Africa.

and surface rainfall, we use the 5-class prognostic Lin microphysics scheme (which includes snow, graupel and mixed-phase processes – Lin et al., 1983). Longwave and shortwave radiation in the model are parametrised by the RRTM (Mlawer et al., 1997) and Goddard shortwave (Chou and Suarez, 1994) schemes respectively. The model domain covers a $2100\,km$ by $2100\,km$ region over
115 the Congo Basin (Fig. 2), chosen due to the highly convective nature of this region and the strong sources of biomass burning aerosol (Fig. 2). The study region incorporates the Congo Basin and a large fraction of the biomass burning region to the north of it (Fig. 2). The model initial and boundary conditions are generated from NCEP reanalysis, starting at 0000 UTC on 01 March 2007 and updated every 6 hours over the three week simulation. The simulation period was selected due
120 to the peak in precipitation in the Congo basin during March and April (Washington et al., 2013).

All of the aerosol in this semi-idealised setup is generated by emissions within the domain. Although simulations of a larger domain (not shown) indicate that a significant amount of the aerosol is transported into the study region from outside, there are sufficient aerosol sources inside the study region so that the influence of precipitation on AOD can be studied. We use the MADE-SORGAM
125 aerosol module (Ackermann et al., 1998; Schell et al., 2001) and include cloud chemistry so that the wet scavenging of aerosols by the stratiform precipitation is represented. This allows aerosols to influence the cloud droplet number concentration. However, the influence of an aerosol indirect effect on the AOD-precipitation relationship in this study is expected to be small compared to wet scavenging. Convective wet scavenging of aerosol is included in the convection scheme. The main variability
130 in emissions over the three week study period comes from biomass burning. Anthropogenic emissions using the EDGAR and RETRO databases and biomass burning emissions using daily updated MODIS fire counts (MCD14ML – Giglio et al., 2003) are generated using PREP-CHEM-SRC (Fre-

5

itas et al., 2011). Biogenic emissions are generated using the Guenther emissions scheme (Guenther et al., 1994), but emissions from biomass burning dominate the AOD in this region.

2.2   Storm composites

To investigate the influence of precipitation on aerosols through wet scavenging, we identify regions of heavy precipitation, specifically convective storms. We then composite these storms, rotating them onto a common direction of travel, so that the properties of these systems and their influence on the AOD can be investigated.

We define our systems using the hourly accumulated precipitation field. We consider a heavy precipitation rate as greater than $2\,mm\,hr^{-1}$, which results in easily separated precipitating systems, without overly restricting the number of these systems. Heavily precipitating, four-connected (two gridboxes are considered joined if they share an edge, not if they only share a corner) gridboxes are then joined together to produce precipitating "blobs".

To determine the direction of travel of a system, the blobs are filtered to select cases that are easy to track, which removes the majority of detected blobs. Only blobs with an area greater than $3,000\,km^2$ and less than $15,000\,km^2$ are retained. Blobs are discarded if they are insufficiently independent of other blobs (forming less than 90% of the precipitating area within 50 km of the blob edge), if they are within 50 km of the domain edge or if they fail to meet circularity criteria. As the blobs are selected to be independent of each other, the position of the blob after one hour is selected as the largest blob within 100 km of the starting position. Over the 21-day simulation, 51444 blobs are found, of which 37 are retained to form the system composite. The direction of travel and velocity are determined from the motion of the storm over a single hour following its detection.

2.3   Observations

The strong link between AOD and CF can generate correlations between AOD and other cloud or precipitation properties (Gryspeerdt et al., 2014a). Here we use the precipitation development method of Gryspeerdt et al. (2014b), which is explicitly designed to account for these covariations, to examine the links between aerosol and precipitation.

The precipitation development method makes use of sub-daily time-resolved precipitation measurements and the diurnal cycle of precipitation, to investigate the link between satellite retrieved aerosol and precipitation. The data are separated into different cloud regimes using the clusters defined in Gryspeerdt and Stier (2012). The high and low aerosol populations are determined as the highest and lowest AOD quartiles for each regime and season. Meteorological covariations and the strong influence of CF are accounted for at the time of the aerosol retrieval (T+0), by ensuring that the high and low AOD populations have the same distribution of CF and meteorological parameters, as described in Gryspeerdt et al. (2014c). This almost completely removes the correlation between AOD and precipitation at T+0, while the different development of precipitation at times before and

after T+0 for the high and low aerosol populations demonstrates the interaction of aerosols with precipitation. This method reduces some of the largest confounding factors when studying aerosol–cloud interactions. A full description of the precipitation development method is given in Gryspeerdt et al. (2014b).

We use precipitation data from the TRMM 3B42 merged precipitation product (Huffman et al., 2007). This product merges precipitation estimates from radar, passive microwave, geostationary infra-red and surface rain gauges to give three-hourly estimates of the precipitation across the tropics. The cloud and aerosol data used are from the MODIS collection 5.1 (Platnick et al., 2003; Remer et al., 2005) level 3 product, with only the dark-target aerosol being used. These data are all gridded to 1° by 1° resolution. To increase the number of available aerosol retrievals in cloudy regions, AOD data is interpolated into gridboxes that have no AOD retrievals if those gridboxes have a neighbour where AOD data exists, following Koren et al. (2012). The interpolation does not generate AOD data for all overcast locations, but it does increase the number of available retrievals in cloudy regions. The MODIS data is used to determine cloud regimes at the time of the aerosol retrieval (T+0), separating cloud with different properties. High aerosol is defined as the highest AOD quartile and low as the lowest quartile. These quartiles are determined for each regime, location and season separately.

Defining the MODIS Aqua overpass time (1330 local solar time – LST) as T+0, we investigate the development of the precipitation for each of the regimes, at times before and after the AOD retrieval. The high and low AOD populations are sampled so that they have the same CF distribution (see. Gryspeerdt et al., 2014c) to remove the AOD–CF relationship at T+0. This is important due to the ability of the AOD–CF correlation to generate correlations between aerosol and other cloud properties (Gryspeerdt et al., 2014a). In this work, we consider only two regimes. The shallow cumulus regime is a low CF regime and the thick mid-level regime is a high CF regime. Both of these regimes showed evidence of the wet scavenging of aerosol and of possible aerosol invigoration of convection in previous work (Gryspeerdt et al., 2014b). It is important to note that the regimes are named for their properties at T+0, as this is when the cloud properties are retrieved. There are often transitions between the regimes over time, so several hours after T+0, a shallow cumulus regime may have transitioned into the deep convective regime (Gryspeerdt et al., 2014c). An increase in precipitation after T+0 in the shallow cumulus regime is likely the result of transitions to more heavily precipitating regimes rather than an increase in precipitation from the shallow cumulus clouds themselves.

As we cannot use satellites to sample aerosol in cloudy regions in the same style as a GCM, we use the ECMWF MACC product (Benedetti et al., 2009) to provide an "all-sky" AOD product. The MACC project assimilates aerosol information from MODIS into the ECMWF integrated forecast system, and so can also provide an AOD estimate in overcast or precipitating scenes where there is no MODIS AOD retrieval. In cloud free regions, MACC is largely similar to MODIS, but as the CF increases, MACC increasingly has to rely on its own modelled estimates of AOD, especially in

205 overcast regions where there are no AOD retrievals to be assimilated. This makes it a suitable replacement for a study using only GCMs, as it provides a model-like "all-sky" AOD for the real world. Due to the resolution of the MACC product and instantaneous mixing of aerosol over each gridbox every timestep, the wet scavenging of aerosols effectively takes place across an entire gridbox. This prevents MACC from providing a separate "clear-sky" AOD..

210 As the MACC AOD product is specified at 0300 UTC (a three hour forecast from 0000 UTC), we interpolate consecutive days to generate a 1330 LST MACC AOD product. Although this interpolated product cannot reproduce the diurnal cycle of AOD, this cycle is much smaller than the diurnal cycle of precipitation (which is captured). Validating MACC (or interpolated MODIS) in cloud covered or precipitating regions is not the focus of this paper. As precipitation in global mod-

215 els can be unrealistic (Stephens et al., 2010), we use the TRMM 3B42 precipitation data to generate precipitation development plots when using the MACC AOD data.
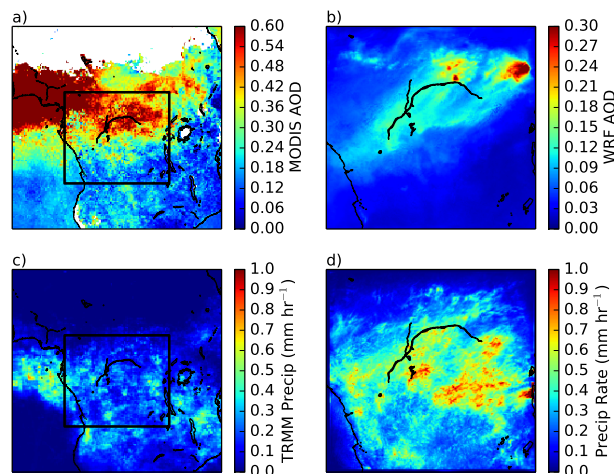
3 Results

3.1 Regional relationships

Figure 3. a) The mean Aqua MODIS AOD in equatorial Africa for March 2007. The box shows the study region. b) The mean AOD at 1330 local time for March 2007 from WRF-Chem. Note the change of color scale. c) The mean TRMM precipitation rate and (d) the mean WRF-Chem precipitation rate for March 2007.

The WRF-Chem simulation shows a strong aerosol plume heading diagonally from north-east
220 (near the main biomass burning regions) to the south-west, following the direction of the prevailing wind (Fig. 3b). With a maximum AOD of around 0.3, this is lower than, although a similar order of magnitude to, the MODIS retrieved AOD. The spatial pattern is similar to MODIS, with a lower AOD in the southern part of the domain, although there is a noticeable difference due to the lack of

aerosol being advected in from outside the domain in WRF-Chem. This semi-idealised setup does not influence our later results, as they depend on the interaction of precipitation and aerosol within the domain.

The precipitation rate in the study region is about double that observed in the TRMM 3B42 product for March 2007 (Figs. 3c,d). However, the spatial pattern shows some similarities, with a reduction of the precipitation towards the north of the domain. The increased precipitation in the model may be partly responsible for the lower AOD in the simulation compared to the MODIS AOD, through an increase in wet scavenging. It is also possible that the use of MODIS fire counts to determine the biomass burning emissions results in an underestimation of the emissions in the southern part of the domain, where cloud cover is higher.

While there are some shortfalls in the representation of the magnitude of the aerosol and precipitation rates in this simulation, the main aim of this work is to investigate the interaction between precipitation and aerosol within the domain. Given the somewhat idealised nature of this study, this simulation represents convective precipitation in an aerosol-laden environment to a sufficient extent for this study.
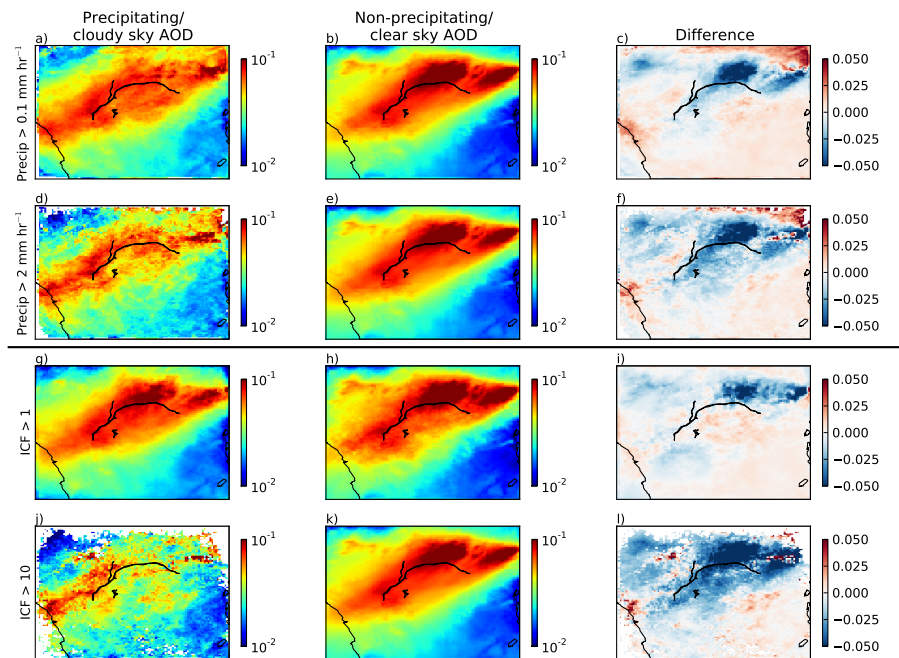

Figure 4. The influence of wet scavenging on AOD in WRF-Chem. Each of the rows uses a different criterion to define clear/cloudy sky. The top two rows use surface precipitation, with precipitation over $0.1\,\mathrm{mm\,hr^{-1}}$ and $2\,\mathrm{mm\,hr^{-1}}$, respectively, defined as cloudy regions. The bottom two rows define cloudy as an integrated cloud flag of greater than 1 and greater than 10 respectively. From left to right, the columns show the cloudy-sky AOD, the clear sky AOD and the difference, with blue indicating a lower AOD in the cloudy sky.

We investigate four different definitions of "precipitating" or "cloudy" when separating the "clear-sky" from the "all-sky" AOD in WRF-Chem. The first two rows in Fig. 4 show definitions of "precipitating" using the WRF-Chem surface precipitation rate. Whilst the "clear-sky" AOD is very similar between the different definitions of "precipitating", the precipitating-sky AOD is much noisier when using the stricter definition ($>2\,\mathrm{mm\,hr^{-1}}$) of "precipitating" (Fig. 4d). For both definitions of "precipitating" (Fig. 4c,f), the AOD in the precipitating scenes is generally lower than that in "clear-sky" scenes. When only heavily precipitating scenes ($>2\,\mathrm{mm\,hr^{-1}}$) are counted as precipitating (Fig. 4f), the reduction in AOD for the precipitating scenes becomes even more pronounced. In regions of significant biomass burning to the north of the domain, part of the reduction in AOD comes from an impact of precipitation on biomass burning emissions. However, large reductions in AOD are also seen in regions further away from aerosol sources, as would be expected if wet scavenging is a major method of removing aerosol (and reducing AOD) in the atmosphere.

The conditions used in the bottom two rows of Fig. 4 are defined using the WRF cloud flag, summed vertically such that it is equal to the number of model layers where there is cloud. This integrated cloud flag (ICF) provides a measure of the geometrical thickness of a cloud. We again find that the "clear-sky" AOD is similar for both the lenient and more stringent cloudiness definitions (Fig. 4h,k) and that as the definition becomes more stringent, the cloudy-sky AOD becomes noisier (Fig. 4j). In general, there is a decrease in AOD in the cloudy scenes compared to the "clear-sky" regions, with this decrease becoming stronger if the cloudiness condition is made more stringent (Fig. 4i,l).

When using either the precipitation or the ICF criteria for separating the "clear-sky" AOD, there are several regions where there is an increase in AOD in the precipitating/cloudy sky, especially when using the less stringent condition (R $>0.1\,\mathrm{mm\,hr^{-1}}$, ICF$>1$). This is primarily due to an increase in relative humidity in these cloudy regions resulting in hygroscopic growth of the aerosols and increasing the AOD (Supplementary Fig. A1). The increase of AOD in cloudy and near-cloud locations is thought to be responsible for a large part of the AOD–CF relationship (Quaas et al., 2010).

3.2 Storm-centric composites

To further investigate the impact of precipitation on aerosol, we examine the properties of a composite of mid-sized convective systems and the surrounding aerosol from our WRF-Chem simulation. Fig. 5a shows a strong reduction in the column integrated AOD where the composite system is currently precipitating and along its previous trajectory (towards the left of the plot). There is also an increase in AOD towards the leading edge of the system, primarily due to aerosol humidification effects (Haywood et al., 1997; Redemann et al., 2009, Supplementary Figs. A2). We also see that both the region where there is a reduction in AOD and that where there is an increase in AOD are obscured by higher cloud cover. As fractional cloud cover is not available in this simulation, f_c is
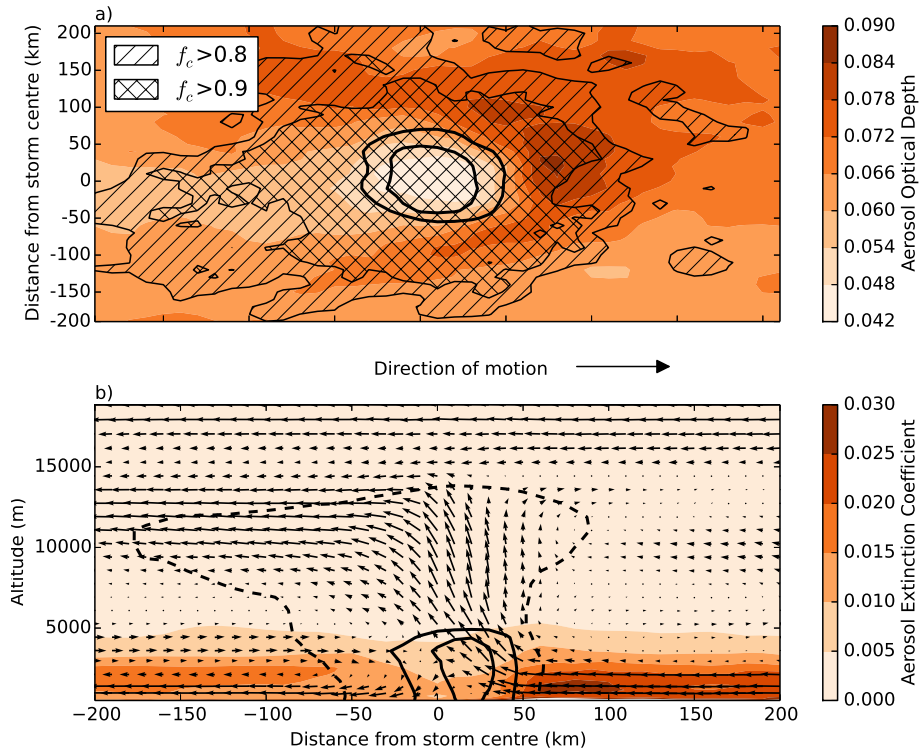
Figure 5. A composite of storms from a three week WRF-Chem simulation in March 2007 over the Congo Basin. The storm composite is moving from left to right on the above plots. *a)* A horizontal plot, with the orange filled contours showing the integrated aerosol optical depth and the hatched regions showing cloud covered regions in 80 and 90% of the storms making up the composite. The solid lines are the 2 and 5 mm hr^{-1} rainrate contours. *b)* A vertical cross section through the centre of the composite storm. The orange contours show the aerosol extinction coefficient and the arrows indicate the wind direction relative to motion of the storm centroid. The vertical wind has been enhanced by a factor of five to compensate for the different vertical and horizontal scales. The solid contours show the 0.2 and 0.8 g kg^{-1} levels of rainwater content and the dashed contour is the -20 dbZ radar reflectivity contour.

the percentage of storms in the composite that have an ICF>1. The region with an f_c of greater than 90% extends slightly in the direction of travel of the system (towards the right of the figure), but trails further behind the system, hiding the main regions where wet scavenging is occurring.

In the vertical cross section (Fig. 5b), we see that the main contribution to the total AOD comes from below 5 km, with only a small amount coming from aerosol being lofted by vertical motion at the leading edge of the system. There is a clear reduction in aerosol in the centre of the system where the most significant precipitation is occurring. The bold black contours showing the location of rainwater within the cloud are displaced slightly from the storm centre, as they are instantaneous

11

values and the storm centre is determined using precipitation values accumulated over one hour periods.

285   We have used the simulated $-20\,\mathrm{dbZ}$ radar reflectivity contour to indicate the edge of the composite system. The storm composite shows a divergent anvil outflow at $10\,\mathrm{km}$ altitude. The $-20\,\mathrm{dbZ}$ contour is also higher directly above the centre of the system, perhaps indicating overshooting tops.

Perhaps most importantly for possible aerosol effects on convective precipitation, the main updraughts in the storm composite contain air that is sourced from ahead of the storm (Fig. 5b). This

290   means that the air ingested by the storm into the updraught areas (where the aerosol activation takes place) has not been affected by precipitation (as would be the case if the storm drew in air from regions it had just passed through). The structure of this composite storm is very similar to that previously observed in radar studies of convective systems (e.g. Houze et al., 1989). The composite displays a 'trailing stratiform' precipitation pattern (where the stratiform precipitation trails the con-

295   vective updraught region), shown by the larger extent of the radar reflectivity and rain water content contours behind the composite storm than in front of it. This structure is more common than the "leading stratiform" structure, where the stratiform precipitation region leads the convective region (Parker and Johnson, 2000). We also observe a weak rear inflow of approximately $4\,\mathrm{ms}^{-1}$ relative to the motion of the composite (Smull and Houze, 1987). This inflow does not reach the centre of the

300   storm, descending to the surface at the trailing edge of the heavily precipitating region (Fig. 5b). The exact structure of the composite depends on the parameters used for selecting the systems making up the composite. Slightly different values can result in a more symmetrical composite system, probably the result of combining leading and trailing stratiform systems. However, the region of main precipitation is still covered by cloud at the centre of the composite.

305   To demonstrate the importance of wet scavenging in reducing the AOD at the centre of the composite convective system. We also examine a composite convective system created from a simulation in which the wet scavenging of aerosols is disabled (Fig. 6). The lack wet scavenging leads to a higher overall AOD, due to the slower rate of aerosol removal. There is an increase in AOD at the centre of the composite system, rather than the decrease in AOD found in Fig. 5, which suggests that

310   wet scavenging is indeed responsible for the reduction in AOD at the centre of the composite system. The increase in AOD at the centre of the composite constructed with wet scavenging absent (Fig. 6) is due to both the hygroscopic growth of the aerosol at the centre of the system and an increase in aerosol dry mass due to aerosol being lofted by the storm.

As this simulation concerns mainly the wet scavenging of boundary layer aerosol, it is possible

315   that the inclusion of free tropospheric aerosol from sources outside the simulation domain might change the relationship between AOD and precipitation in the composite. However, Grandey et al. (2014) showed that convective wet scavenging of aerosol is responsible for generating a negative AOD-precipitation correlation in a GCM throughout the tropics, even far from the main sources
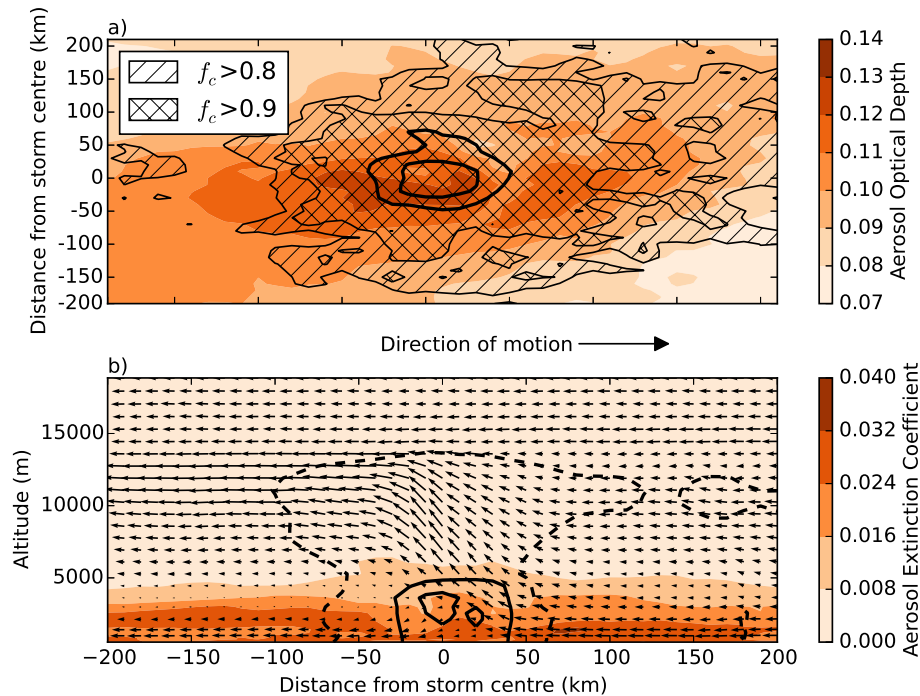
Figure 6. As Fig. 5 but constructed from a simulation with no wet scavenging of aerosol. This composite is composed of 22 individual convective systems.

of aerosol. This would suggest that including free tropospheric aerosol this simulation would not
320 impact the simulated AOD-precipitation relationships.

A simulation with a resolution of 10 km may not be able to resolve all of the important features in the convective systems that are part of this composite. However, the composite shows a qualitative similarity with a composite generated from a simulation at 4 km resolution without chemistry or aerosols (see Supplementary Information Section B). The updraughts are in the same location at the
325 front of the storm, drawing in air from regions that have not previously experienced precipitation.

4 Observational Consequences

Large differences between clear-sky and all-sky aerosol relating to the occurrence of precipitation have been observed in the WRF-Chem simulation. However, it is unclear to what extent the inability to distinguish clear-sky and all-sky aerosol might impact observed aerosol–cloud–precipitation rela-
330 tionships. In this section, we use two aerosol products to investigate the importance of distinguishing the "clear-sky" AOD (MODIS AOD) from the "all-sky" AOD (MACC AOD) for observed aerosol–cloud–precipitation relationships. While the previous section has only shown the difference of the
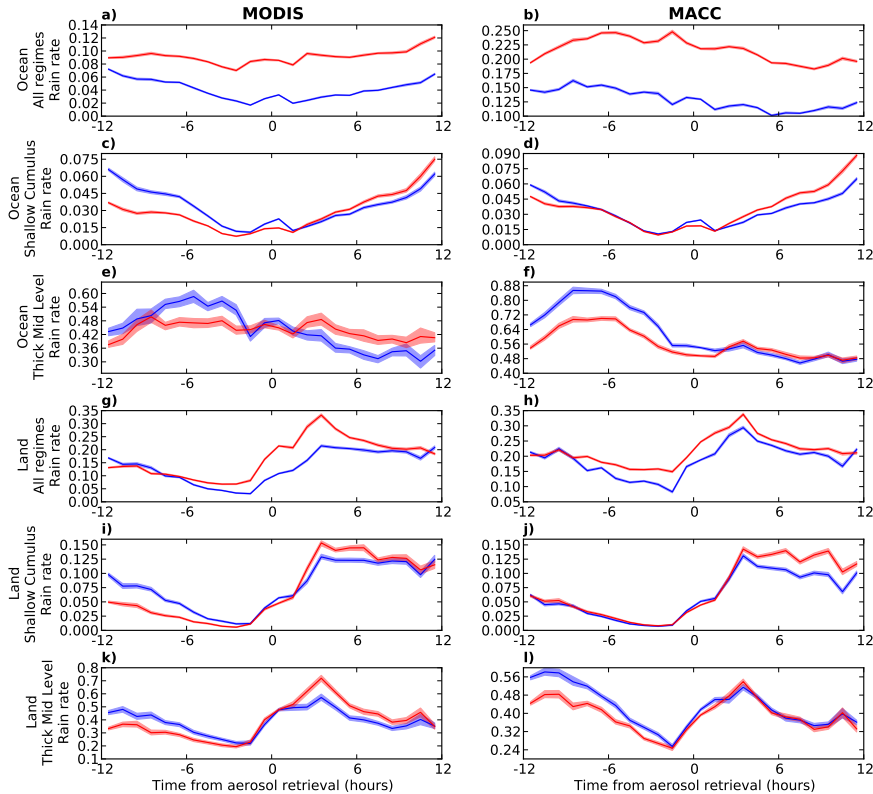
Figure 7. TRMM 3B42 precipitation development plots in the style of Gryspeerdt et al. (2014b) from 2003–2007 between 30°N and 30°S, comparing the use of MODIS AOD (left column) and MACC Total AOD at 550 nm (right column) as the aerosol product. This shows the development of the precipitation at times before and after the aerosol retrieval (1330 LST). The red line is the precipitation rate for the high AOD population and the blue for the low AOD population. Statistical errors are shown at the 95 % level. The plots are shown for ocean (a–f) and land (g–l) separately. For each product and surface type, data for all the regimes together is shown along with the shallow cumulus regime (as an example of a low CF regime) and the thick mid-level regime (as an example of a high CF regime). The cloud regimes are only specified at the time of the aerosol retrieval; transitions may occur between regimes at other times. TRMM 3B42 merged precipitation is used throughout this figure.

"clear-sky" and the "all-sky" AOD in the Congo Basin region, previous work using global models has indicated that they are important to distinguish throughout the tropics (Grandey et al., 2014).

335   While some differences between the "all-sky" MACC AOD and the "clear-sky" MODIS AOD are shown in Fig. 1, the strong impact of aerosol humidification on the relationship obscures a possible influence of aerosol on precipitation. We use the precipitation development method from Gryspeerdt et al. (2014a) to reduce the influence of these meteorological covariations on the AOD-precipitation relationship while retaining the ability to detect a possible influence of aerosol on precipitation.

14

340   We find strong similarities in the precipitation development of the different cloud regimes when using MACC AOD and MODIS AOD (Fig. 7). When regimes and CF variations are not considered, both MODIS (Fig. 7a) and MACC (Fig. 7b) AOD show a strong link between precipitation and AOD over ocean, before, at and after T+0. This relationship is also seen over land, although to a lesser extent (Fig. 7g,h), with increased precipitation from the high AOD population (red line) compared to

345   the low AOD population. This matches the effect seen in Fig. 1, where increased AOD is correlated to an increase in retrieved precipitation.

    The diurnal cycle of precipitation is very similar between the plots using MODIS AOD and using MACC AOD, as the same precipitation dataset is used for both sets of plots. The absolute magnitude of the precipitation is larger when using MACC AOD, as MACC allows the sampling of overcast

350   regions with a higher precipitation rate that MODIS cannot sample.

    In the shallow cumulus regime (a low CF regime), the "all-sky" AOD is dominated by the "clear-sky" AOD. When using MODIS AOD (Fig. 7c,i), we see a higher precipitation rate for the low AOD population compared to the high AOD population at times before T+0, previously interpreted as wet scavenging (Gryspeerdt et al., 2014b). We also see an increase in the precipitation rate for the

355   high AOD population compared to the low AOD population at times after T+0, over both land and ocean. This may indicate an aerosol invigoration of convective clouds (Gryspeerdt et al., 2014b). It is important to note that the cloud regime is only determined at T+0, with transitions between regimes occurring at other times. As such, the apparent invigoration of the shallow cumulus regime is not necessarily due to a change in precipitation from shallow cumulus clouds, but is likely due to

360   transitions into more heavily precipitating regimes (Gryspeerdt et al., 2014c).

    When comparing the precipitation development plots using MACC AOD (Fig. 7d,j) to those using MODIS AOD, the shallow cumulus regime shows similar features. The increase in precipitation for the high AOD population compared to the low AOD population is still visible after T+0 over land. However, there is very little difference in the precipitation rate at times before T+0 between the high

365   and low AOD populations (Fig. 7d,j). This contrasts strongly with the MODIS AOD results, where a wet scavenging signature is easily visible over both land and ocean for the shallow cumulus regime.

    The thick mid-level regime is an example of a high CF regime, where MODIS AOD retrievals are less common and the "clear-sky" AOD is a much smaller proportion of the "all-sky" AOD. For both MODIS (Fig. 7e,k) and MACC (Fig. 7f,l) we see a higher precipitation rate for the low AOD

370   population before T+0, over both land and ocean. This indicates the wet scavenging of aerosol. The higher precipitation rates when using MACC AOD over ocean (Fig. 7f) are likely due to the increased sampling of overcast, precipitating locations that MACC allows for. The higher precipitation rate from the low AOD population before T+0, consistent with wet scavenging, is observed when using both MACC and MODIS AOD, an increase in precipitation with increasing AOD after T+0 is only

375   observed when using MODIS AOD. This increase in precipitation with increasing AOD observed when using MODIS is consistent with an aerosol invigoration of convective clouds. If this increase

in precipitation is due to an aerosol invigoration effect, then this suggests that the use of MACC AOD obscures the aerosol influence on precipitation in these high CF, highly precipitating regimes.

5 Discussion

5.1 "All-sky" vs. "Clear-sky" AOD

The analysis of AOD for different precipitation rates in Fig. 4 generally shows a reduced AOD in cloudy/precipitating areas. The high CF in these locations would restrict the satellite retrieval of AOD. This can also be seen on the scale of an individual storm in the storm composite (Fig. 5), where the AOD is reduced in the precipitating region towards the centre of the storm. This reduction in AOD would be hard to retrieve with satellites due to the high cloud cover, while the AOD in lower f_c regions towards the edge of the storm has not been so strongly influenced by precipitation, remaining similar to the "clear-sky" AOD at the edge of the composited region.

This provides further evidence that the difference in the AOD–precipitation correlation between MODIS and the HadGEM-UKCA GCM shown in Fig. 1 is due to differences in sampling between the model and observations, as suggested in Grandey et al. (2014). In regions with a high precipitation rate (such as the tropics), wet scavenging dominates over aerosol hygroscopic growth when determining the relationship between the "all-sky" AOD and precipitation, explaining the negative correlation in Fig. 1c. Wet scavenging impacts the "clear-sky" aerosol via the post-storm "wake" that can be seen to the left of Fig. 5a. Although this "wake" would be visible to satellites, it is a very small proportion of the "clear-sky" aerosol when compared to the impact of wet scavenging on aerosol in the cloud covered regions of the composite. This means that precipitation exerts a much stronger control over the aerosol in cloudy regions compared to the "clear-sky" aerosol. As the "clear-sky" aerosol is not so heavily scavenged, wet scavenging does not play such a strong role in determining the correlation between "clear-sky" AOD and precipitation. In these situations, the influence of aerosol hygroscopic growth is more important (Boucher and Quaas, 2012; Grandey et al., 2014), generating much of the positive correlation between AOD and precipitation seen in Fig. 1c.

While the correlations in Fig. 1 show the link between AOD and precipitation, they cannot provide evidence of aerosol invigoration of convective clouds due to the confounding effects of meteorological covariations (Boucher and Quaas, 2012; Grandey et al., 2013; Gryspeerdt et al., 2014c). The precipitation development plots in this work are designed to account for the influence of meteorological covariations when investigating aerosol–cloud interactions. The observation of both wet scavenging and possible aerosol invigoration when using MODIS suggests that aerosol invigoration could be responsible for an increase in precipitation from convective clouds under certain conditions (Gryspeerdt et al., 2014b). The increase in precipitation after T+0 and the wet scavenging effect are only observed in certain regimes when using MACC aerosol data. Given the different sampling of

16

MACC and MODIS AOD, this suggests that the strong effect of wet scavenging on AOD in cloudy skies might be obscuring an aerosol influence on precipitation in some regimes.

In heavily precipitating regions, the "all-sky" AOD observed by a model (with a similar sampling to MACC) is significantly lower than the "clear sky" AOD, as seen in the WRF-Chem results (Fig. 4). A lower AOD is not itself enough to prevent the observation of an aerosol invigoration effect in the precipitation development plots, as they depend on the AOD having some predictive power of the future evolution of the storm, rather than the absolute magnitude of the AOD. However, in regions of high CF and strong precipitation, the "all-sky" AOD–precipitation correlation is controlled almost entirely by wet scavenging. In these regions, the control of the aerosol by precipitation means that the "all-sky" AOD then loses its predictive power over the future evolution of the storm, only reflecting the previous history of the airmass. This suggests that the "clear-sky" AOD, preferentially sampled by satellites, is more representative of the aerosol environment in the early stages of the formation of storms, as it is not so strongly affected by precipitation from those storms. While the influence of wet scavenging can affect satellite studies (Fig. 7), low resolution models are much more significantly affected as they are less able to separate the "clear-sky" aerosol from the "all-sky" aerosol.

The mixing of clear and cloudy sky aerosol populations explains why the wet scavenging of aerosols is visible in the precipitation development plots from the thick mid-level regime (high CF) when using MACC AOD but the increase in precipitation with increasing AOD after T+0 is not visible. In this high CF regime, the MACC AOD is strongly influenced by the model precipitation, as there are few MODIS AOD retrievals to assimilate. The MACC AOD is then much more strongly connected to the history of the precipitation rate than it is to the aerosol that is drawn into the cloud, preventing the apparent invigoration of the thick mid-level regime over land (Fig. 7k) from being observed using MACC AOD (Fig. 7l).

In low CF regimes (such as the shallow cumulus), this is not an issue as the majority of the aerosol is "clear-sky" aerosol and so the "all-sky" AOD closely tracks the "clear-sky" AOD. This allows the observation of an apparent invigoration of precipitation from the shallow cumulus regime when using both MACC (Fig. 7i) and MODIS AOD (Fig. 7j).

Wet scavenging obscuring the influence of aerosols on convective clouds also explains some of the results in previous work. Gryspeerdt et al. (2014c) investigated the links between aerosols and transitions between cloud regimes, finding that whilst increased transitions to deep convective-type clouds were observed with increases in MODIS aerosol index, this increase was not observed when using MACC AOD. The results in this work suggest that this is most likely due to the influence of wet scavenging and the sampling difference between MACC and MODIS AOD.

The influence of wet scavenging does not need to have a large effect on the total mean AOD to have a strong effect on the link between AOD and precipitation development within the strongly precipitating/high CF regimes. These high CF/strongly precipitating regimes occur rarely, with only 13% of the cloud regime occurring in the tropics falling into the deep convective or thick mid-

level regimes (Gryspeerdt and Stier, 2012). Even though the sampling varies between MACC and MODIS, the mean MACC AOD is very close to that determined using MODIS and other satellite instruments (Morcrette et al., 2011). This demonstrates that although the overall magnitude of the wet scavenging in MACC may be similar to that seen in observations, small sampling differences can impact correlations between aerosol and cloud properties.

5.2 Comparison to GCM processes

We have shown that the clear-sky sampling bias in satellite AOD data impacts the correlations between AOD and precipitation. Both the composite storm in Fig. 5 and previous radar-based studies of convective systems suggest that air is usually drawn into convective updraughts from non-precipitating regions. Coupled with the reduction in aerosol in cloudy skies due to wet scavenging, this suggests that the "clear-sky" AOD could be more closely related to the aerosol drawn into convective systems than the "all-sky" AOD (which is more strongly influenced by precipitation). GCMs assume that aerosol is mixed across a gridbox on a timescale of a model timestep (10–30 minutes), limiting their ability to distinguish the "clear-sky" aerosol from the "all sky" aerosol. This may make it difficult for GCMs to detect aerosol influences on precipitation using the precipitation development method.

A preference for using the "clear-sky" aerosol when investigating aerosol–cloud interactions is not likely to be the case for all precipitating clouds. As shown in previous work, models can reproduce the observed AOD–CF correlation more successfully in mid-latitude regions than they can near the equator (Grandey et al., 2014). This suggests that this sampling difference is not as important an issue where frontal precipitation is involved, perhaps due to the larger precipitation spatial scales involved. The intensity of the precipitation involved is also important, as the precipitation must be intense enough to remove the link between the "all-sky" and the "clear-sky" aerosol. Unlike the convective regimes, the development of the stratocumulus regime shows a similar correlation to MACC AOD as it does to MODIS AOD (Gryspeerdt et al., 2014c), suggesting that the "all-sky" and the "clear-sky" aerosol are correlated for cloud regimes with low precipitation rates.

The storm composite in Fig. 5 is composed of storms approaching the size of a GCM gridbox that are independent from other storm systems. The filtering techniques used to select the storms for the storm composite may have introduced a bias into the composite so that is it not representative of convective storms in general. As noted earlier, the storm composite displays the more common trailing stratiform structure. However, leading stratiform structure storms may ingest air into convective updraughts from locations with recent precipitation or through the stratiform precipitation regions, reducing the link between the "clear-sky" AOD and the ingested aerosol. The requirement that the storms be independent of neighbouring precipitating systems may also bias the structure of the composite. In large groups of interacting individual convective systems, new systems may be triggered by the outflow from convective downdraughts (Thorpe et al., 1982; Wakimoto, 1982).

18

This makes new convective systems more likely to ingest air that is part of the outflow from other systems. As the aerosol in the outflow has come from inside a cloud, the "all-sky" sampling may be more representative of the aerosol ingested by convective systems in these cases.

While there are some cases where the "clear-sky" AOD may not have an advantage over the "all-sky" AOD, the precipitation development results (Fig. 7) suggest that the "clear-sky" AOD has an advantage in detecting influences of aerosol on precipitation. If the "clear-sky" AOD can not be separated from the "all-sky" AOD, links between aerosol and precipitation development from convective systems can be obscured. Due to the difficulty in determining the "clear-sky" AOD in GCMs, this is may impact the detectability of aerosol influences on precipitation in GCMs using the precipitation development method.

6 Conclusions

In this work we have used the WRF-Chem model and satellite observations to examine how aerosol is affected in precipitating convective systems and how this impacts correlations between AOD and precipitation properties.

Using the WRF-Chem model, we have found that there is generally a reduction in AOD in precipitating regions (Fig. 4), with this reduction becoming more severe when more stringent conditions are used to define precipitating regions. We also find a decrease in AOD in cloud covered locations, due to the strong link between CF and precipitation in the Congo region. In scenes with a low (but non-zero) precipitation rate, there is an increase in AOD with increasing precipitation, primarily caused by the hygroscopic growth of aerosol in humid environments (Supplementary Fig. A1).

Creating a composite of mid-sized convective systems in our study region (Fig. 5), we show how aerosol interacts with precipitating systems on the storm scale. AOD is strongly reduced in the core of these systems, where the precipitation is strongest, although the reduction in AOD persists in locations where the system has previously been precipitating. The regions where the most significant reduction in AOD occurs are in locations that are usually covered by cloud, preventing their observation by satellites. This results in different sampling of AOD between satellites and models and help to explain the difference in the AOD–precipitation correlation between them (Fig. 1).

The composite also shows how air is drawn into convective systems relative to their direction of travel, such that the aerosol ingested by a system has not previously interacted with precipitation from the same storm system. This suggests that the aerosol drawn into such storm systems is more closely related to the "clear-sky" AOD observed by satellites than the "all-sky" AOD that is sampled by atmospheric models. The importance of the "clear-sky" aerosol relative to the "all-sky" aerosol varies by cloud regime, but for sufficiently spaced individual convective systems as analysed here, this would suggest that the satellite "clear-sky" sampling of AOD may be more suited to investigating aerosol–cloud interactions.

This is supported by observations using MODIS AOD and the TRMM merged precipitation product, along with MACC reanalysis AOD to provide a model-like "all-sky" AOD field. When looking at two specific regimes, the shallow cumulus (with a low CF) and the thick mid-level (with a high CF), we see an invigoration-like effect in both regimes when using MODIS AOD. When using MACC AOD, we only see the invigoration-like effect in the low CF regime, suggesting that the use of "all-sky" AOD in highly precipitating regimes masks the observation of a possible invigoration effect.

This work shows that the different sampling of aerosols by satellites and reanalysis models/GCMs can have a large effect on the correlations between aerosol and precipitation properties. When using the precipitation development method in highly-precipitating convective regimes, an increase in precipitation with increasing AOD seen when using MODIS AOD cannot be detected when using MACC reanalysis AOD. This suggests that even if a GCM has a perfect representation of aerosol effects on convective clouds, it may not be able to reproduce the correlations between AOD and precipitation in highly precipitating locations, due to the differences in AOD sampling between GCMs and satellites.

References

Ackermann, I. J., Hass, H., Memmesheimer, M., Ebel, A., Binkowski, F. S., and Shankar, U.: Modal aerosol dynamics model for Europe, Atm. Env., 32, 2981–2999, doi:10.1016/S1352-2310(98)00006-5, 1998.

Albrecht, B.: Aerosols, Cloud Microphysics, and Fractional Cloudiness, Science, 245, 1227–1230, doi:10.1126/science.245.4923.1227, 1989.

Andreae, M. and Rosenfeld, D.: Aerosol cloud precipitation interactions. Part 1. The nature and sources of cloud-active aerosols, Earth Sci. Rev., 89, 13–41, doi:10.1016/j.earscirev.2008.03.001, 2008.

Benedetti, A., Morcrette, J.-J., Boucher, O., Dethof, A., Engelen, R. J., Fisher, M., Flentje, H., Huneeus, N., Jones, L., Kaiser, J. W., Kinne, S., Mangold, A., Razinger, M., Simmons, A. J., and Suttie, M.: Aerosol analysis and forecast in the European Centre for Medium-Range Weather Forecasts Integrated Forecast System: 2. Data assimilation, J. Geophys. Res., 114, D13 205, doi:10.1029/2008JD011115, 2009.

Boucher, O. and Quaas, J.: Water vapour affects both rain and aerosol optical depth, Nat. Geosci., 6, 4–5, doi:10.1038/ngeo1692, 2012.

Chand, D., Wood, R., Ghan, S. J., Wang, M., Ovchinnikov, M., Rasch, P. J., Miller, S., Schichtel, B., and Moore, T.: Aerosol optical depth increase in partly cloudy conditions, J. Geophys. Res., 117, D17207, doi:10.1029/2012JD017894, 2012.

Chou, M.-D. and Suarez, M. J.: An efficient thermal infrared radiation parameterization for use in general circulation models, in: NASA Tech. Memo, p. 84, 1994.

Freitas, S. R., Longo, K. M., Alonso, M. F., Pirre, M., Marecal, V., Grell, G., Stockler, R., Mello, R. F., and Sánchez Gácita, M.: PREP-CHEM-SRC - 1.0: a preprocessor of trace gas and aerosol emission fields for regional and global atmospheric chemistry models, GeoSci. Mod. Dev., 4, 419–433, doi:10.5194/gmd-4-419-2011, 2011.

Giglio, L., Descloitres, J., Justice, C. O., and Kaufman, Y. J.: An Enhanced Contextual Fire Detection Algorithm for MODIS, Remote Sens. Environ., 87, 273–282, doi:10.1016/S0034-4257(03)00184-6, 2003.

Grandey, B. S., Stier, P., and Wagner, T. M.: Investigating relationships between aerosol optical depth and cloud fraction using satellite, aerosol reanalysis and general circulation model data, Atmos. Chem. Phys., 13, 3177–3184, doi:10.5194/acp-13-3177-2013, 2013.

Grandey, B. S., Gururaj, A., Stier, P., and Wagner, T. M.: Rainfall-aerosol relationships explained by wet scavenging and humidity, Geophys. Res. Lett., 41, 5678–5684, doi:10.1002/2014GL060958, 2014.

Grell, G. A.: A generalized approach to parameterizing convection combining ensemble and data assimilation techniques, Geophys. Res. Lett., 29, doi:10.1029/2002GL015311, 2002.

Grell, G. A., Peckham, S. E., Schmitz, R., McKeen, S. A., Frost, G., Skamarock, W. C., and Eder, B.: Fully coupled "online" chemistry within the WRF model, Atmos. Env., 39, 6957–6975, doi:10.1016/j.atmosenv.2005.04.027, 2005.

Gryspeerdt, E. and Stier, P.: Regime-based analysis of aerosol-cloud interactions, Geophys. Rev. Lett., 39, L21802, doi:10.1029/2012GL053221, 2012.

Gryspeerdt, E., Stier, P., and Grandey, B.: Cloud fraction mediates the aerosol optical depth - cloud top height relationship, Geophys. Rev. Lett., 41, doi:10.1002/2014GL059524, 2014a.

Gryspeerdt, E., Stier, P., and Partridge, D.: Links between satellite retrieved aerosol and precipitation, Atmos. Chem. Phys., 14, 9677–9694, doi:10.5194/acp-14-9677-2014, 2014b.

21

Gryspeerdt, E., Stier, P., and Partridge, D. G.: Satellite observations of cloud regime development: the role of aerosol processes, Atmos. Chem. Phys., 14, 1141–1158, doi:10.5194/acp-14-1141-2014, 2014c.

Guenther, A., Zimmerman, P., and Wildermuth, M.: Natural volatile organic compound emission rate estimates for U.S. woodland landscapes, Atm. Env., 28, 1197–1210, doi:10.1016/1352-2310(94)90297-6, 1994.

585 Haywood, J. M., Ramaswamy, V., and Donner, L. J.: A limited-area-model case study of the effects of sub-grid scale Variations in relative humidity and cloud upon the direct radiative forcing of sulfate aerosol, Geophys. Res. Lett., 24, 143–146, doi:10.1029/96GL03812, 1997.

Houze, R. A., Biggerstaff, M. I., Rutledge, S. A., and Smull, B. F.: Interpretation of Doppler Weather Radar Displays of Midlatitude Mesoscale Convective Systems, Bull. Am. Met. Soc., 70, 608–619, doi:10.1175/1520-
590 0477(1989)070<0608:IODWRD>2.0.CO;2, 1989.

Huffman, G. J., Bolvin, D. T., Nelkin, E. J., Wolff, D. B., Adler, R. F., Gu, G., Hong, Y., Bowman, K. P., and Stocker, E. F.: The TRMM Multisatellite Precipitation Analysis (TMPA): Quasi-Global, Multiyear, Combined-Sensor Precipitation Estimates at Fine Scales, J. Hydrometeorology, 8, 38–55, doi:10.1175/JHM560.1, 2007.

595 Jethva, H., Torres, O., Waquet, F., Chand, D., and Hu, Y.: How do A-train sensors intercompare in the retrieval of above-cloud aerosol optical depth? A case study-based assessment, Geophys. Res. Lett., 41, 186–192, doi:10.1002/2013GL058405, 2014.

Khain, A., Rosenfeld, D., and Pokrovsky, A.: Aerosol impact on the dynamics and microphysics of deep convective clouds, Q. J. RMetS., 131, 2639–2663, doi:10.1256/qj.04.62, 2005.

600 Koren, I., Altaratz, O., Remer, L. A., Feingold, G., Martins, J. V., and Heiblum, R. H.: Aerosol-induced intensification of rain from the tropics to the mid-latitudes, Nature Geosci., 5, 118, doi:10.1038/ngeo1364, 2012.

Li, Z., Niu, F., Fan, J., Liu, Y., Rosenfeld, D., and Ding, Y.: Long-term impacts of aerosols on the vertical development of clouds and precipitation, Nat. Geosci., 4, 888, doi:10.1038/ngeo1313, 2011.

605 Lin, J., Matsui, T., Pielke, R., and Kummerow, C.: Effects of biomass-burning-derived aerosols on precipitation and clouds in the Amazon Basin: A satellite-based empirical study, J. Geophys. Res., 111, D19 204, doi:10.1029/2005JD006884, 2006.

Lin, Y.-L., Farley, R. D., and Orville, H. D.: Bulk Parameterization of the Snow Field in a Cloud Model, J. Clim. App. Met., 22, 1065–1092, doi:10.1175/1520-0450(1983)022<1065:BPOTSF>2.0.CO;2, 1983.

610 Mann, G., Johnson, C., Bellouin, N., Dalvi, M., Abraham, L., Carslaw, K. S., Boucher, O., Stier, P., Rae, J., Spraklen, D. V., Telford, P., Pyle, J., O'Connor, F., Carver, G., Pringle, K. J., and Woodhouse, M. T.: Evaluation of the new UKCA climate– composition model. Part 3:Tropospheric aerosol properties, in preparation, 2014.

Mauger, G. and Norris, J.: Meteorological bias in satellite estimates of aerosol-cloud relationships, Geophys.
615 Rev. Lett., 34, D16824, doi:10.1029/2007GL029952, 2007.

Mlawer, E. J., Taubman, S. J., Brown, P. D., Iacono, M. J., and Clough, S. A.: Radiative transfer for inhomogeneous atmospheres: RRTM, a validated correlated-k model for the longwave, J. Geophys. Res., 102, 16 663, doi:10.1029/97JD00237, 1997.

Morcrette, J.-J., Benedetti, A., Jones, L., Kaiser, J., Razinger, M., and Suttie, M.: Prognostic aerosols in the
620 ECMWF IFS: MACC vs GEMS aerosols, Tech. rep., ECMWF, Reading, UK, 2011.

Nakajima, T., Higurashi, A., Kawamoto, K., and Penner, J.: A possible correlation between satellite-derived cloud and aerosol microphysical parameters, Geophys. Res. Lett., 28, 1171–1174, doi:10.1029/2000GL012186, 2001.

Niu, F. and Li, Z.: Systematic variations of cloud top temperature and precipitation rate with aerosols over the global tropics, Atmos. Chem. Phys., 12, 8491–8498, doi:10.5194/acp-12-8491-2012, 2012.

Parker, M. D. and Johnson, R. H.: Organizational Modes of Midlatitude Mesoscale Convective Systems, M. Weather Rev., 128, 3413–3436, doi:10.1175/1520-0493(2001)129<3413:OMOMMC>2.0.CO;2, 2000.

Platnick, S., King, M., Ackerman, S., Menzel, W., Baum, B., Riedi, J., and Frey, R.: The MODIS cloud products: algorithms and examples from Terra, IEEE T. GeoSci. Remote, 41, 459, doi:10.1109/TGRS.2002.808301, 2003.

Quaas, J., Stevens, B., Stier, P., and Lohmann, U.: Interpreting the cloud cover - aerosol optical depth relationship found in satellite data using a general circulation model, Atmos. Chem. Phys., 10, 6129–6135, doi:10.5194/acp-10-6129-2010, 2010.

Redemann, J., Zhang, Q., Russell, P. B., Livingston, J. M., and Remer, L. A.: Case studies of aerosol remote sensing in the vicinity of clouds, J. Geophys. Res., 114, D06 209, doi:10.1029/2008JD010774, 2009.

Remer, L., Kaufman, Y., Tanré, D., Matto, S., Chu, D., Martins, J., Li, R.-R., Ichoku, C., Levy, R., Kleidman, R., Eck, T., Vermote, E., and Holben, B.: The MODIS aerosol algorithm, products, and validation, J. Atmos. Sci., 62, 947–973, doi:10.1175/JAS3385.1, 2005.

Rosenfeld, D., Lohmann, U., Raga, G., O'Dowd, C., Kulmala, M., Fuzzi, S., Reissell, A., and Andreae, M.: Flood or Drought: How Do Aerosols Affect Precipitation?, Science, 321, 1309–1313, doi:10.1126/science.1160606, 2008.

Schell, B., Ackermann, I. J., Hass, H., Binkowski, F. S., and Ebel, A.: Modeling the formation of secondary organic aerosol within a comprehensive air quality model system, J. Geophys. Res., 106, 28 275–28 293, doi:10.1029/2001JD000384, 2001.

Smull, B. F. and Houze, R. A.: Rear Inflow in Squall Lines with Trailing Stratiform Precipitation, M. Weather Rev., 115, 2869–2889, doi:10.1175/1520-0493(1987)115<2869:RIISLW>2.0.CO;2, 1987.

Stephens, G., L'Ecuyer, T., Forbes, R., Gettlemen, A., Golaz, J.-C., Bodas-Salcedo, A., Suzuki, K., Gabriel, P., and Haynes, J.: Dreary state of precipitation in global models, J. Geophys. Res., 115, D24 211, doi:10.1029/2010JD014532, 2010.

Stevens, B. and Feingold, G.: Untangling aerosol effects on clouds and precipitation in a buffered system, Nature, 461, 607–613, doi:10.1038/nature08281, 2009.

Stier, P., Feichter, J., Kinne, S., Kloster, S., Vignati, E., Wilson, J., Ganzeveld, L., Tegen, I., Werner, M., Balkanski, Y., Schulz, M., Boucher, O., Minikin, A., and Petzold, A.: The aerosol-climate model ECHAM5-HAM, Atmos. Chem. Phys., 5, 1125, doi:10.5194/acp-5-1125-2005, 2005.

Tao, W.-K., Li, X., Khain, A., Matsui, T., Lang, S., and Simpson, J.: Role of atmospheric aerosol concentration on deep convective precipitation: Cloud-resolving model simulations, J. Geophys. Res., 112, D24S18, doi:10.1029/2007JD008728, 2007.

Textor, C., Schulz, M., Guibert, S., Kinne, S., Balkanski, Y., Bauer, S., Berntsen, T., Berglen, T., Boucher, O., Chin, M., Dentener, F., Diehl, T., Easter, R., Feichter, H., Fillmore, D., Ghan, S., Ginoux, P., Gong, S., Grini, A., Hendricks, J., Horowitz, L., Huang, P., Isaksen, I., Iversen, I., Kloster, S., Koch, D., Kirkevåg,

23

A., Kristjansson, J., Krol, M., Lauer, A., Lamarque, J., Liu, X., Montanaro, V., Myhre, G., Penner, J., Pitari, G., Reddy, S., Seland, Ø., Stier, P., Takemura, T., and Tie, X.: Analysis and quantification of the diversities of aerosol life cycles within AeroCom, Atmos. Chem. Phys., 6, 1777–1813, doi:10.5194/acp-6-1777-2006, 2006.

665 Thorpe, A. J., Miller, M. J., and Moncrieff, M. W.: Two-dimensional convection in non-constant shear: A model of mid-latitude squall lines, Q. J. RMetS., 108, 739–762, doi:10.1002/qj.49710845802, 1982.

Twomey, S.: Pollution and the Planetary Albedo, Atm. Env., 8, 1251–1256, doi:10.1016/0004-6981(74)90004-3, 1974.

Wakimoto, R. M.: The Life Cycle of Thunderstorm Gust Fronts as Viewed with Doppler Radar and Rawinsonde

670 Data, M. Weather Rev., 110, 1060–1082, doi:10.1175/1520-0493(1982)110<1060:TLCOTG>2.0.CO;2, 1982.

Washington, R., James, R., Pearce, H., Pokam, W. M., and Moufouma-Okia, W.: Congo Basin rainfall climatology: can we believe the climate models?, Phil. Trans. R. Soc. B, 368, 20120 296, doi:10.1098/rstb.2012.0296, 2013.

675 Wen, G., Marshak, A., Cahalan, R., Remer, L., and Kleidman, R.: 3-D aerosol-cloud radiative interaction observed in collocated MODIS and ASTER images of cumulus cloud fields, J. Geophys. Res., 112, D13204, doi:10.1029/2006JD008267, 2007.

Williams, E., Rosenfeld, D., Madden, N., Gerlach, J., Gears, N., Atkinson, L., Dunnemann, N., Frostrom, G., Antonio, M., Biazon, B., Camargo, R., Franca, H., Gomes, A., Lima, M., Machado, R., Manhaes, S.,

680 Nachtigall, L., Piva, H., Quintiliano, W., Machado, L., Artaxo, P., Roberts, G., Renno, N., Blakeslee, R., Bailey, J., Boccippio, D., Betts, A., Wolff, D., Roy, B., Halverson, J., Rickenbach, T., Fuentes, J., and Avelino, E.: Contrasting convective regimes over the Amazon: Implications for cloud electrification, J. Geophys. Res., 107, 8082, doi:10.1029/2001JD000380, 2002.

Winker, D., Hunt, W., and McGill, M.: Initial performance assessment of CALIOP, Geophys. Res. Lett., 34,

685 L19 803, doi:10.1029/2007GL030135, 2007.

Zhang, J., Reid, J., and Holben, B.: An analysis of potential cloud artifacts in MODIS over ocean aerosol optical thickness products, Geophys. Res. Lett., 32, L15803, doi:10.1029/2005GL023254, 2005.